Journal of Mechatronics, Electrical Power, and Vehicular Technology

Geometrical and dimensional tolerance analysis for the radial flux type of permanent magnet generator design

Muhammad Fathul Hikmawan [a, b], Agung Wibowo [b, *], Muhammad Kasim [a, c]

[a] Research Centre for Electrical Power and Mechatronics, Indonesian Institute of Sciences
Komp LIPI Jl. Sangkuriang, Building 20, 2nd Floor, Bandung, West Java, 40135, Indonesia

[b] Faculty of Mechanical and Aerospace Engineering, Bandung Institute of Technology
Jl. Ganesa No.10, Lb. Siliwangi, Bandung, 40132, Indonesia

[c] School of Electrical Engineering and Telecommunications, University of New South Wales
330 Anzac Parade, Kensington NSW 2033, Australia

Abstract

Mechanical tolerance is something that should be carefully taken into consideration and cannot be avoided in a product for manufacturing and assembly needs, especially in the design stage, to avoid excessive dimensional and geometric deviations of the components made. This paper discusses how to determine and allocate dimensional and geometric tolerances in the design of a 10 kW, 500 rpm radial flux permanent magnet generator prototype components. The electrical and mechanical design results in the form of the detailed nominal dimensions of the generator components, and the allowable air gap range are used as input parameters for tolerance analysis. The values of tolerance allocation and re-allocation process are carried out by considering the capability of the production machine and the ease level of the manufacturing process. The tolerance stack-up analysis method based on the worst case (WC) scenario is used to determine the cumulative effect on the air gap distance due to the allocated tolerance and to ensure that the cumulative effect is acceptable so as to guarantee the generator's functionality. The calculations and simulations results show that with an air gap of 1 ± 0.2 mm, the maximum air gap value obtained is 1.1785 mm, and the minimum is 0.8 mm. The smallest tolerance value allocation is 1 μm on the shaft precisely on the FSBS/SRBS feature and the rotor on the RPMS feature. In addition, the manufacturing process required to achieve the smallest tolerance allocation value is grinding, lapping, and polishing processes.

I. Introduction

The world has switched to using renewable energy in the face of the energy crisis and global warming. A permanent magnet generator (PMG) is a device that converts mechanical energy into electrical energy. The advantages of PMG are high efficiency, can be designed for low rotation, compact construction, and easy maintenance. It cannot be denied that PMG is suitable to be applied as a renewable energy power plant [1][2] as well as to be applied to electric and hybrid vehicles [3]. Research and development about this generator are still being carried out now, such as research on design optimization conducted by [4] and on a wind power generation system with a magnetic generator.

Reference [5] seeks to optimize the power generation system of small-scale wind turbines. This system also uses a permanent magnet synchronous generator, which is connected directly to the turbine. The optimization of PMG with an interior type rotor or often called an interior permanent magnet synchronous generator (IPMSG) for applications in electric vehicles has been carried out by [6].

Several studies on the design of radial type permanent magnets for renewable energy generation applications have been carried out by [7][8][9]. The result of the design is in the form of detailed dimensions of the stator and rotor. Considerations regarding the tolerance of generator components in the design have not been much done, although this tolerance is very important to be taken into account at the design stage.

The manufacturing process is one of the stages to realize the product design. In most cases of

generator manufacturing, mechanical tolerances inevitably occur because of the need for manufacturing and assembly processes. The tolerance influences the performance of the permanent magnet generator. The production process of permanent magnet generators and the effect on their general characteristics have been described by [10]. Many studies have been carried out to investigate the impact of mechanical tolerance on electrical parameters. Reference [11] has conducted a sensitivity analysis to determine its impact on the electrical parameters of PMG using the finite element method (FEM) by changing the design variable in the range of tolerance values. Research to investigate the effect of tolerances and manufacturing limits on permanent magnet generators with large dimensions has also been carried out by [12]. The analysis was carried out using a method that combines the FE method with direct superposition. Reference [13] investigated the impact of this mechanical tolerance by measuring the magnetic flux density and the length of the air gap, as well as the magnetization and the permanent magnet size. Meanwhile, reference [14] conducted research on cogging torque caused by manufacturing tolerances using analytical methods, finite element analysis (FEA), and experimental methods. Among the results, it is known that the tolerance of the stator inner diameter has the greatest influence on the cogging torque in the stator. While in the rotor, permanent magnet remanence is the main contributor, followed by the thickness of the magnet and the tolerance of the outer radius of the rotor. From these studies, it can be concluded that the most basic parameters of a permanent magnet electric machine are closely related to the mechanical tolerance of the air gap.

Tolerance stack-up analysis is a method used to determine the cumulative effect of tolerances allocated to the features of a component and to ensure that the cumulative effect is acceptable to ensure product functionality after an assembly process [15]. The tolerance stack-up analysis method is generally divided into two basic methods, namely the worst-case (WC)-based and statistical-based analysis or also known as the root sum of the square (RSS). The combination method between WC and RSS gave birth to the modified root sum of the square (MRSS) method. The comparison of the three methods is seen from the aspect of the risk of production defects; the WC method is the lowest, followed by MRSS and RSS is the highest. However, if viewed from the cost side, it is the opposite, where the WC method is the highest and RSS is the lowest. Other basic statistical methods that have been developed are the six sigma method, genetic algorithm (GA), and Monte Carlo simulation. Six sigma method was first introduced by the Motorola Company [16]. GA is an adaptive experience search algorithm based on the evolutionary ideas of natural selection. The steps of using this GA method have been described by [17]. Meanwhile, the Monte Carlo simulation method is based on randomness. This method is used to generate random variables for analysis in various fields for nonlinear engineering

models. GA and Monte Carlo simulation are quite powerful methods for optimization. The main drawback of both methods is that they require a lot of computation to get acceptable accuracy from statistically significant results. At the same time, the advantage is that the results obtained are more optimal than other statistical methods. Several ways to overcome the weaknesses of these methods, as well as the weaknesses of the worst-case and statistical-based tolerance analysis methods, have been proposed, one of which is the analytical method introduced by [18]. Another method of dimensional and geometrical tolerance analysis was introduced by [19]. The uncertainty of the dimensions and geometry of a component feature is packaged in a mathematical form with fuzzy modeling and the kinematic effect of tolerance in a product assembly is expressed by a concept called the small degrees of freedom (SDOF) concept. The method commonly used for tolerance analysis is the Monte Carlo simulation [20]. However, a lot of software has been developed based on this method. research conducted by [21] in their paper describes the use of Knowledge Based Engineering (KBE) to adjust tolerances based on the functional requirements of a product. The calculation and analysis of tolerances in the design of marine engine transmissions are carried out using software, that is, integrated computer aided design (CAD) and computer aided tolerancing (CAT) based on the Monte Carlo method. The results of the study indicate that KBE can be useful for driving tolerance changes towards values that ensure optimal functionality of the assembly. Research on tolerance stack analysis on a Francis turbine design by [22] using the worst case (WC) method with consideration of the number of products produced and the need to ensure 100 % correctness on each dimension of its components.

This paper discusses how to determine and allocate tolerances in the prototype components design of a 10 kW, 500 rpm permanent magnet generator with radial flux type. The distribution flow of the relationship between the component features that play a role in compiling the key characteristics (KC) of the permanent magnet generator will be identified and mapped as an effort to control tolerances from the design stage, the production process, to the component inspection stage after production. Consideration of the ability of production machines in the tolerance allocation process can provide an overview of the sequence of component manufacturing processes in real terms. Tolerance stack-up analysis to determine the cumulative effect on the air gap distance due to the allocated tolerance uses manual analytical simulation based on the worst case (WC) method, where dimensional tolerances and geometry are taken into account simultaneously. This method is chosen because it is suitable for product design in the prototype stage, that is, the number of products to be made is small and the risk of manufacturing defects is the smallest. Another advantage of using this method is that the analysis can be carried out easily and with simple equipment.

II. Materials and Methods

The results of the electrical and mechanical design in the form of details of the component's nominal dimensions, as well as the allowable range of air gaps used as input parameters for tolerance analysis, are shown in Table 1. This tolerance analysis process is carried out at the final stage of mechanical design before entering the generator prototype manufacturing/production process.

Tolerance analysis of the 10 kW, 500 rpm permanent magnet generator prototype design was carried out in two stages, namely the identification stage and the analysis and calculation stages. The identification stage is carried out to find out the features of the components that contribute to compiling KC. The analysis and calculation stages are carried out to ensure the cumulative effect of each tolerance allocated to the component features that contribute to the KC is following the allowable requirements.

A. Tolerance chain

The air gap is a key characteristic (KC), which is structurally located on the radial axis outside the shaft rotation. Analysis of tolerance propagation that affects the value of KC can be observed from the relationship between the features of its constituent components. The structure of the generator arrangement drawing shown in Figure 1 shows the identifying the features process of the components that contributes to compiling KC and the relationship between the features of these components. The red line in the figure is the relationship between the corresponding component features. The first adjustment is between the stator outer surface (SOS) feature and the stator surface frame (SSF). The second adjustment is between the

Table 1.
Tolerance analysis input parameter

Component	Component's feature	Value (mm)
Stator	Diameter of stator outer surface (SOS)	337
	Diameter of stator inner surface (SIS)	400
	Stator effective length (L_i)	85
Rotor	Diameter of rotor permanent magnet surface (RPMS)	323
Shaft	Diameter of front/rear-surface bearing shaft (F/R-SBS)	75
Magnet	Magnet height (h_M)	6
	Magnet width (l_M)	63,5
	Radius of magnet outer surface (MOS)	167,5
	Radius of magnet bottom surface (MBS)	161,5
Air gap	Air gap (g)	1
	Allowable deviation of air gap ($\triangle g$)	± 0,2
Bearing	Diameter of inner bearing surface (IBS)	75
	Diameter of outer bearing surface (OBS)	130
Frame	Diameter of stator surface frame (SSF)	400
	Diameter of front/rear-surface frame (F/R-SF)	412
End-Shield	Diameter of bearing surface end-shield (BSE)	130
	Diameter of frame surface end-shield (FSE)	412

front surface frame (FSF) and the rear surface frame (RSF) with the frame surface end-shield (FSE). The third adjustment is between the bearing surface end-shield (BSE) and the outer bearing surface (OBS).
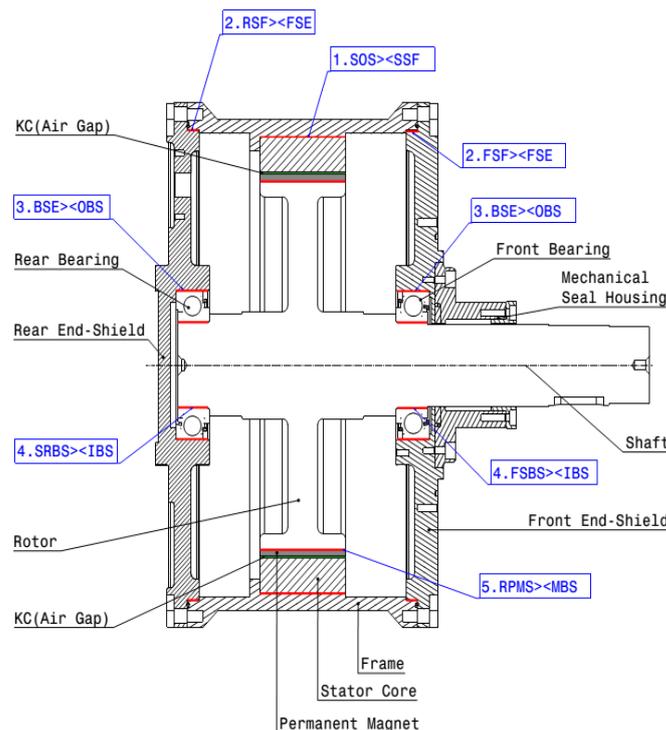
Figure 1. Component features identification
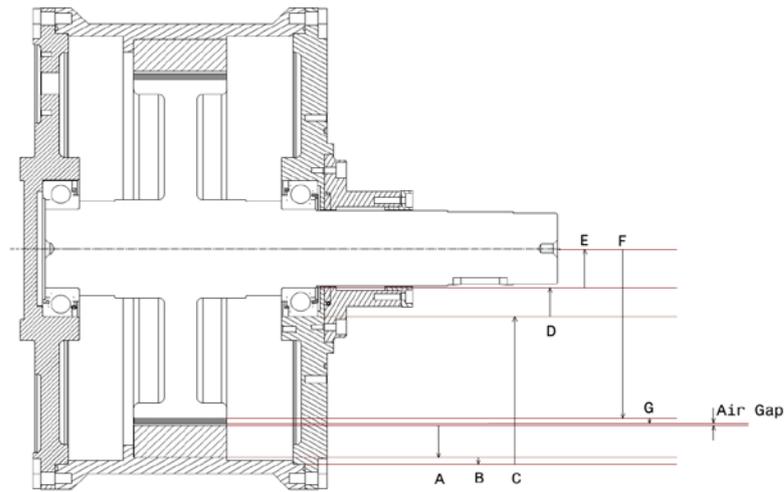
Figure 2. Loop diagram analysis of air gap variation
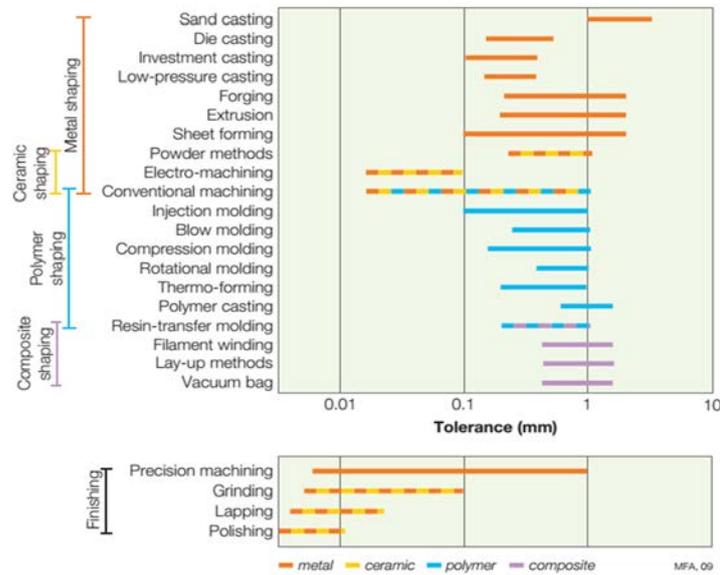
Figure 3. Tolerance chart in manufacturing process selection [23]

The fourth adjustment is between the front shaft bearing surface (FSBS) and the shaft rear bearing surface (SRBS) with the inner bearing surface (IBS). The fifth adjustment is between the rotor permanent magnet surface (RPMS) and the magnet bottom surface (MBS). The features of these intersecting components must be controlled by allocating dimensional tolerances and specifying precise geometric tolerances.

The identification results of the component features that contribute to compiling this KC will be obtaining a schematic relationship between components to create a loop diagram. Figure 2 shows a loop diagram which is a closed graphical representation of the tolerance propagation chain of each contributor/variable KC, which is useful for analysing the calculation of tolerance accumulation in the air gap. From the figure, it can be seen that there are seven variables A to G, which will affect the accumulated tolerance value in the air gap. The actual value of each of these variables will be influenced by the dimensions and geometry tolerances allocated to each contributor component feature.

B. Tolerance allocation

The tolerance allocation process is the process of distributing the allowable requirements to KC, which in this case is the air gap to each contributor component feature. The allocated tolerances consist of dimensional tolerances and geometric tolerances. From Table 1, it is known that the allowable deviation of the air gap (Δg) is $\pm$ 0.2 mm. This value is obtained from the optimization results in the final stage of electrical design using the finite element analysis (FEA) method. It has been confirmed that with a deviation of $\pm$ 0.2 mm in the air gap, it has been ensured that the magnetic flux distribution and cogging torque values are still within the expected design performance. If the value of the allowable air gap requirement is 1±0.2 mm, then the total accumulated dimension and geometric tolerances allocated to each contributor component feature are a maximum of 1.2 mm or a minimum of 0.8 mm.

The first step of tolerance allocation is to consider the ability of the production machine, in particular, the ability of the machine to achieve the allocated tolerance value. Figure 3 shows a graph of

Table 2.
Fits types between component features

No	Fits		Function
	Feature	Type	
1	SOS-SSF	Transition fit	The stator must be firmly attached to the frame, but can still be removed for maintenance purposes
2	FSF-FSE/RSF-RSE	Transition fit	The end shield must be firmly attached to the body, but can still be removed for maintenance purposes
3	BSE-OBS	Clearance fit	Bearing load is balanced with inner ring/rotating shaft section and static outer ring
4	FSBS/SRBS-IBS	Interference fit	Bearing load is balanced with inner ring/rotating shaft section and static outer ring ring
5	RPMS-MBS	no	Fixed permanently

Table 3.
Base hole fit selection system

Basic hole	Tolerance classes for shafts														
	Clearance fits				Transition fits						Interference fits				
h6					g5	h5	js5	k5	m5		n5	p5				
h7				f6	g6	h6	js6	k6	m6	n6		p6	r6	s6	t6	u6	x6
h8			e7	f7			h7	js7	k7	m7				s7		u7
		d8	e8	f8			h8									
h9			d8	e8	f8			h8								
h10	b9	c9	d9	e9	f9			h9								
h11	b11	c11	d11				h10									

the tolerance values that can be achieved using some commonly used manufacturing process/machine methods. The process of making magnets is carried out by a powder metallurgy process followed by a surface finishing process by a grinding process. The minimum tolerance value allocation is 0.02 mm. This magnetic tolerance value is assumed to be a fixed value due to the consideration that the manufacturing process is relatively difficult and expensive. The process of making the stator is in electro machining process with wire cutting. In the process of making the stator, what must be considered is to maintain the insulating layer on the surface of each laminate layer so that it is not damaged. Therefore, additional finishing processes obtaining tight tolerance values are not recommended. For this reason, the stator tolerance value is also assumed to be a fixed value, with the minimum allocation value being 0.02 mm, according to the maximum capacity of the wire cut machine. The manufacturing process for other components such as the Rotor-Shaft, Generator body/Frame, and End-Shield cover is carried out by conventional machining processes. To achieve the tolerance value, it can be done with a finishing process using grinding, lapping, or polishing so that the tolerance allocation process for these components will be more flexible.

The second step of the tolerance allocation process is to determine the type of fits between the contributing component's features in terms of function. Each type of fits between the contributing component's features is shown in Table 2. After knowing each type of adjustment, the dimensional tolerance value of the corresponding features can be determined using the principle of the base hole system. Table 3 shows a base hole-based dimensional tolerance value selection system according to the ISO 286-1.2010 standard.

In Table 2, in the 5th fits between the RPMS and MBS features there is no fits type because it is not included in the fits type based on the base hole or base shaft fits. So, the determination of the tolerance value that is allocated is only based on the ability of the production machine.

The third step is to allocate geometric tolerances to each component feature that contributes to the accumulation of KC tolerances. In determining the type of geometric tolerance, two things must be considered, namely the air gap requirements and the assembly requirements between components in terms of geometry. Judging from the air gap requirements, the position of the rotating axis of the rotor with the stator must be one axis / coaxial. These conditions must be able to be maintained by the bearing, body cover, and generator body together so that the air gap distance will always be the same along the surface between the rotor and the stator. Meanwhile, if viewed from the aspect of assembly between components, it must be considered is the tolerance of the shape, position, or location of the component features that will match each other. For example, the geometric tolerance between the hole and the axis, then at least the spherical or cylindrical tolerance between the two must be taken into account.

C. Component feature deviation analysis

The deviation analysis process is carried out by simulating the deviation of the contributor component features after the dimensions and geometry tolerances have been allocated. The simulation will be useful to make it easier to formulate calculations in finding variable values. The simulation process can be done using any CAD software, but in this study, the software used is solidwork. Figure 4 shows the allocation of geometric tolerances on the stator for SOS and SIS features.
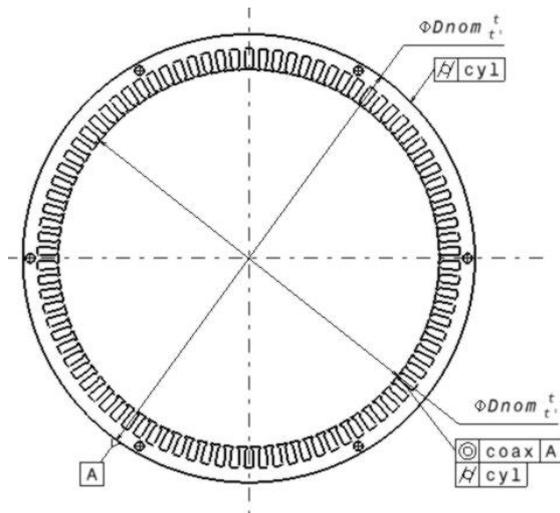
Figure 4. Allocation of stator geometry tolerances on SOS and SIS features

A proper understanding of the allocated geometry tolerance is crucial in the process of simulating the feature deviation. From Figure 4, the SOS feature axis was chosen as the primary datum because the surface of this feature will later sit on the frame. This feature surface is allocated a cylindrical tolerance, which means that every point on the feature surface must be in a space bounded by two coaxial imaginary cylindrical casings spaced as the value of the tolerance (cyl). In the SIS feature, the coaxiality geometry tolerances for datum A and cylindricity tolerance are allocated. The meaning of coaxiality tolerant is that each point of observation of the centre circle diameter/axis of the SIS features must be within the tolerance area in the form of a cylinder with a diameter value of the tolerance (coax), which is made based on the centre axis of the diameter of the SOS feature/datum A. Then, a simulation drawing of the deviation of each feature is made based on understanding the meaning of its geometric tolerance zone. The deviation simulation can be seen in Figure 5. The maximum deviation condition for the SIS feature occurs when the centre point of the feature experiences a maximum shift from its coaxial tolerance value (coax) and every point on the feature surface is at the upper limit of its cylindrical tolerance value (cyl). The minimum deviation of the SIS features occurs when the

Figure 6. Allocation of geometry tolerances on the frame

axis/centre point of the feature circle is in accordance with datum A/coaxiality tolerance is 0 mm (coax = 0) and every point on the inner diameter surface is at the lower limit of its cylindrical tolerance value (cyl). For the SOS feature, the maximum deviation occurs when every point on the outer diameter surface is at the upper limit of the cylindrical tolerance value, while the minimum deviation occurs when every point on the surface of the outer diameter is at the lower limit of the cylindrical tolerance value (cyl).

The next geometric tolerance allocation is also allocated to other components. Figure 6 is an allocation of geometric tolerances in the frame for FSF/RSF and SSF features. The FSF and RSF feature axes are used together as the primary H-I datum. The three features are equally allocated coaxiality and cylindrical tolerances. Aberration simulations are depicted in Figure 7 for deviations in FSF/RSF features. The minimum and maximum deviation conditions that occur in the FSF/RSF feature are similar to the SIS feature on the stator component. Likewise, the deviation conditions that occur in SSF features as shown in Figure 8.

Figure 5. Stator features deviation simulation
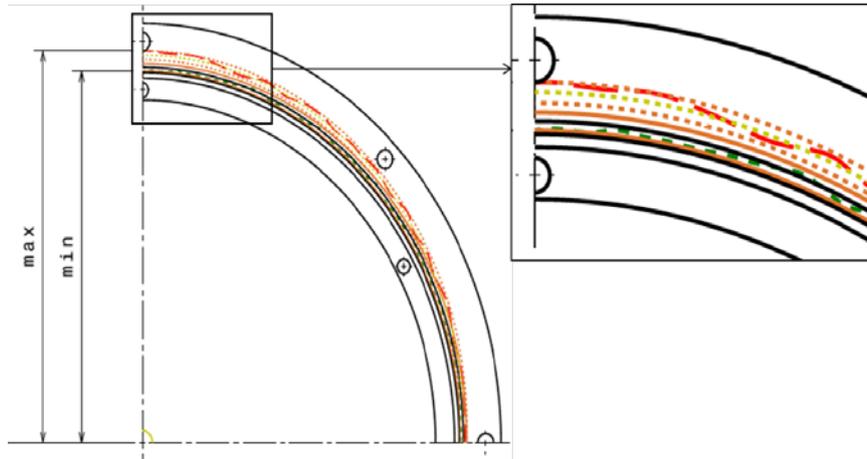
Figure 7. FSF/RSF feature deviation simulation
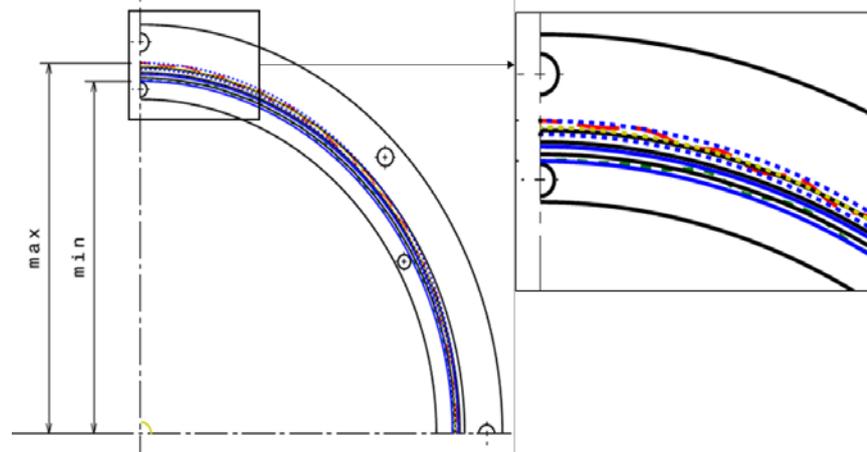
Figure 8. SSF feature deviation simulation

In the body cover/end-shield component, the allocation of geometric tolerances can be seen in Figure 9. The BSE feature axis is selected as the primary datum with the symbol G. This feature is allocated a cylindrical tolerance. For the FSE feature, the coaxiality tolerance for datum G and cylindricity is allocated.

The minimum and maximum deviation conditions that occur in the BSE feature are similar to the condition of the SOS feature on the stator component. Meanwhile, the deviation condition of the FSE feature has similarities with the SIS Stator and FSF/RSF Frame features. Figure 10 shows a simulation of the deviation of the BSE and FSE features.

For the tolerance value, the dimensions and geometry of the standard bearing components are selected based on the bearing specifications used. In this generator design, the bearing used is a deep groove ball bearing type 6215, with nominal dimensions of 75 mm inner diameter, 130 mm outer diameter and 25 mm thickness. The tolerance value can be selected according to the bearing class. Table 4 shows the tolerance specifications for ball bearings according to the bearing class.

The maximum and minimum deviations of the OBS and IBS bearing features can be seen in Figure 11. The deviation conditions of these features are similar to the SOS features on the stator, where the maximum deviation occurs when every point on the outer diameter surface is at the upper limit of its geometric tolerance value. And vice versa for the minimum conditions. From the simulation of the maximum and minimum deviation conditions, an equation can be formulated to calculate the deviation value of these features. To distinguish
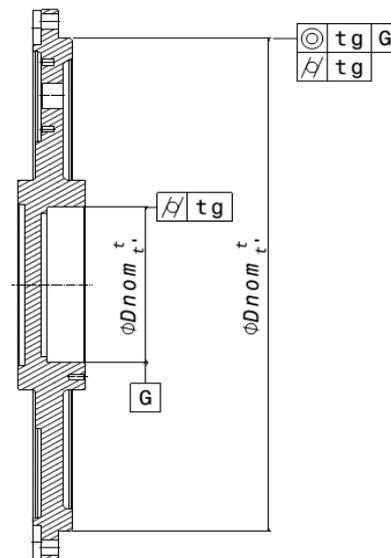
Figure 9. Allocation of geometry tolerances on BSE dan FSE end-shield features

feature deviations from components that have two features under review, the smaller diameter features is given the symbol "ftr" and the larger diameter features are given the symbol "Ftr". Then the equations for the minimum and maximum deviation of features are as follows:

$$Ftr_{min} = ftr_{min} = \frac{(D_{nom}+t'-cyl)}{2} \qquad (1)$$

$$Ftr_{max} = ftr_{max} = \frac{(D_{nom}+t+coax+cyl)}{2} \qquad (2)$$

where Ftr_{min} is minimum deviation of larger diameter features, Ftr_{max} is maximum deviation of

larger diameter features, ftr_{min} is minimum deviation of smaller diameter features, ftr_{max} is maximum deviation of smaller diameter features, *Dnom* is nominal value of feature diameter, t is dimensional tolerance of the upper limit of the feature, and t' is the lower limit, *cyl* is cylindrical tolerance, *coax* is coaxiality tolerance.

Furthermore, to find the nominal value of the variables A, B, C, and D, the maximum condition of the variable material *(V2$_{MMC}$)* and the minimum condition of the stator material *(V2$_{LMC}$)* are calculated first. Because the variable distance A to D
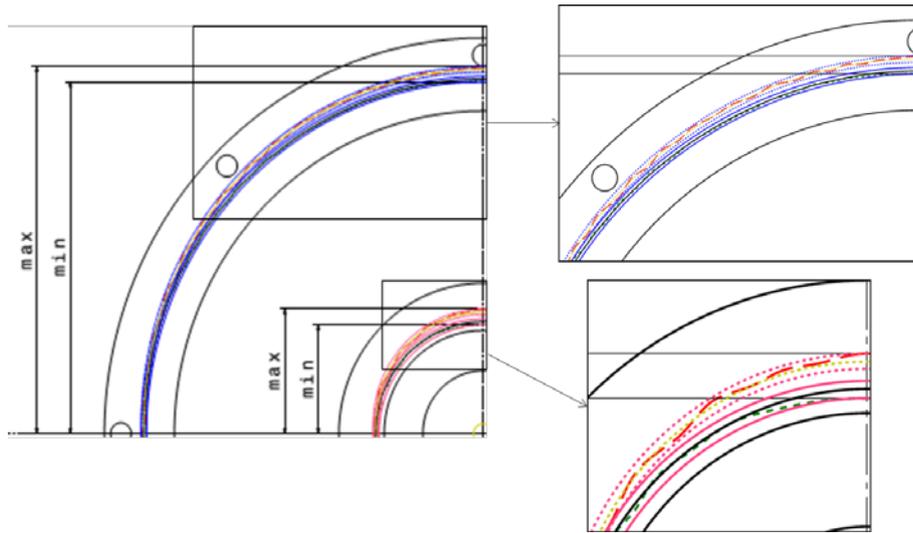
Figure 10. BSE dan FSE feature deviation simulation
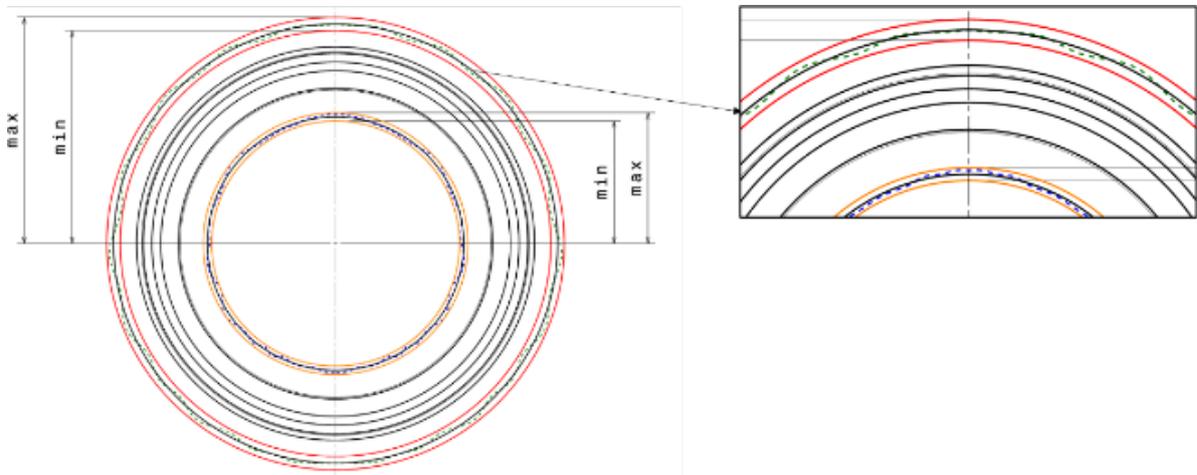
Figure 11. OBS dan IBS feature deviation simulation

Table 4.
Bearing tolerance specifications [24]

Tolerance	Features	Class 0		Class 6		Class 5		Class 4		Class 2	
		(+)	(-)	(+)	(-)	(+)	(-)	(+)	(-)	(+)	(-)
		(μ m)									
Dimension	Inner ring	0	-15	0	-12	0	-9	0	-7	0	-4
	Outer ring	0	-18	0	-15	0	-11	0	-9	0	-5
	Width	0	-120	0	-120	0	-120	0	-120	0	-120
Geometry	Inner ring	15		10		5		4		2,5	
	Outer ring	25		13		8		5		4	
	Side inner	no		no		8		4		2,5	
	Side outer	no		no		10		5		4	
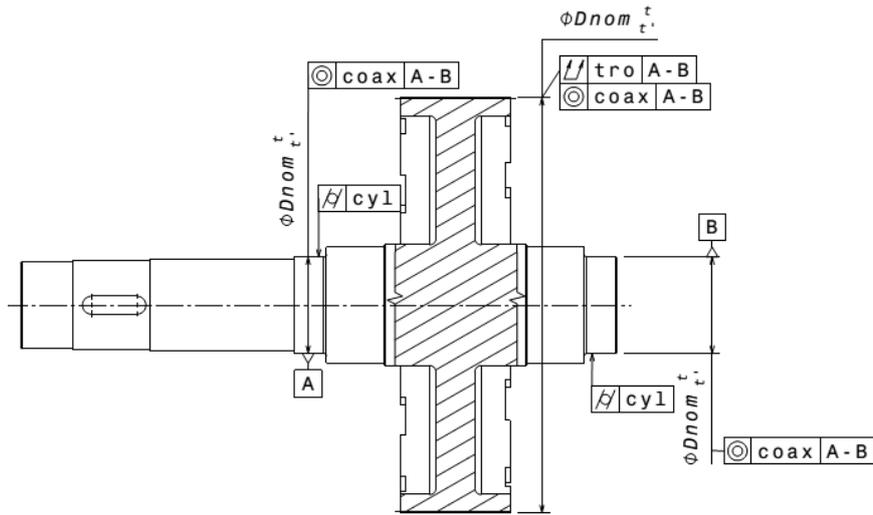
Figure 12. Allocation of geometry tolerances FSBS/SRBS shaft feature and RPMS rotor features
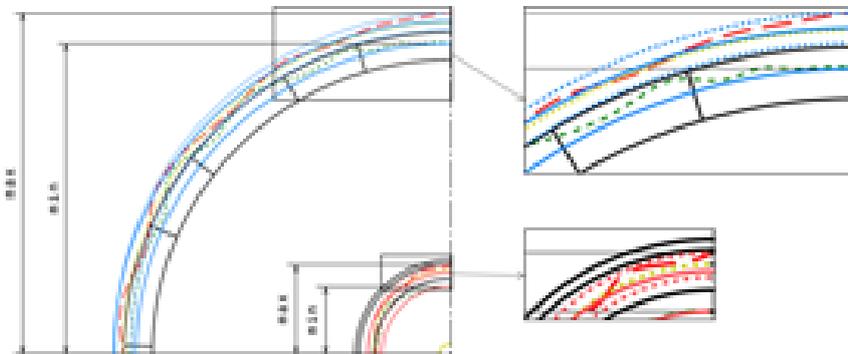
Figure 13. FSBS/SRBS shaft features and RPMS rotor features deviation simulation

is the distance between the two component features, the $V2_{MMC}$ and $V2_{LMC}$ can be calculated respectively by the equations:

$$V2_{MMC} = \frac{(Ftr_{max} - ftr_{min})}{2} \tag{3}$$

$$V2_{LMC} = \frac{(Ftr_{min} - ftr_{max})}{2} \tag{4}$$

Furthermore, the nominal value of the variables A, B, C and D (V_{A-D}) as well as the bilateral equal tolerance value (T_{A-D}) can be obtained by the following equations:

$$V_{A-D} = \frac{(V2_{MMC} + V2_{LMC})}{2} \tag{5}$$

$$T_{A-D} \pm= \frac{(V2_{MMC} - V2_{LMC})}{2} \tag{6}$$

Each of the Shaft and Rotor components has only one feature to be reviewed because the other features are the axes of the feature. For the allocation of geometry tolerances for the shaft FSBS/SRBS feature and the rotor RPMS feature, see Figure 12. The shaft FSBS/SRBS feature axes are together used as primary datums A-B. Each axis feature is allocated a coaxiality geometry tolerance to the A-B datum and the cylindrical.

Furthermore, a simulation of the deviation of these features is carried out. Figure 13 shows a simulation of the deviation of the features of the shaft and rotor components. The maximum and minimum deviation conditions that occur also have

similarities with the features of the SIS Stator. So to calculate the maximum deviation (Ftr_{max}) and minimum (Ftr_{min}) of the shaft FSBS/SRBS feature and the rotor RPMS feature, one can use equations (1) and 2.

Meanwhile, the nominal value of the variables E and F (V_{E-F}) and the bilateral equal tolerance value (T_{E-F}) can be directly calculated by the following equations:

$$V_{E-F} = \frac{((Ftr_{max} + Ftr_{min})}{2} \tag{7}$$

$$T_{A-D} \pm= \frac{((Ftr_{max} - Ftr_{min})}{2} \tag{8}$$

For permanent magnet components, the allocation of geometric tolerances can be seen in Figure 14, while the deviation simulation of the outer surface (MOS) and bottom surface (MBS) magnets can be seen in Figure 15.

From the deviation simulation, if the geometry tolerance allocated to the surface of the two features is the surface accuracy $(surf)$, the maximum (Ros_{max}) and minimum (Ros_{min}) deviations of the MOS and MBS features can be calculated by the following equations:

$$Ros_{min} = D_{nom} + t' + (\tfrac{1}{2} surf) \tag{9}$$

$$Ros_{max} = D_{nom} - t - (\tfrac{1}{2} surf) \tag{10}$$
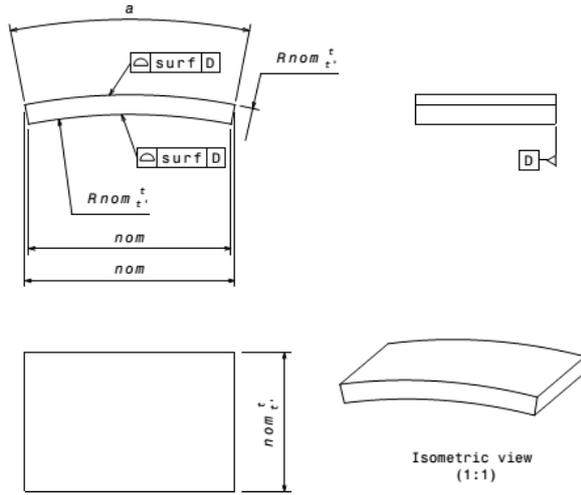
Figure 14. Allocation of magnetic geometry tolerance

The value of the loop variable G and its tolerance is calculated by first calculating the maximum material condition *(G_MMC)* and the minimum material condition *(G_LMC)* magnet, with the equations:

$$G_{MMC} = \frac{(Ros_{max}+Ris_{min})}{2} \tag{11}$$

$$G_{LMC} = \frac{(Ros_{min}-Ris_{max})}{2} \tag{12}$$

So, that the nominal value of the variable (VG) and its tolerance *(T_G)* can be obtained by the following equations:

$$V_G = \frac{(G_{MMC}+G_{LMC})}{2} \tag{13}$$

$$T_G \pm = \frac{(G_{MMC}-G_{LMC})}{2} \tag{14}$$

D. Calculation of accumulated tolerance

The accumulated tolerance/total tolerance *(Tt)* on the air gap is calculated using the worst-case method, with the following equation:

$$Tt = Tol_1 + Tol_2 + \cdots + Tol_n = \sum_{i=1}^{n} Tol_i \tag{15}$$

where $\pm Tol_i$ is the tolerance value of the ith dimension in equal-bilateral format.

According to the loop diagram in Figure 2, the direction of tolerance propagation for variables with a downward vector direction *(V_y)*, namely A, B, F and G is given a negative sign (-), because if the distance value of each variable is increased, it will cause a reduction in the air gap distance. On the other hand, the variables with upward vector directions *(V_x)*, namely C, D and E, are given a positive sign (+)

Table 5.
Resizing priority order

Priority	Component	Features
1	Rotor	RPMS
2	Shaft	FSBS-RSBS
3	End-Shield	FSE
4	Frame	FSF-RSF
5	End-Shield	SSF
6	Bearing	—

because if the distance of each variable increases, it will cause an increase in the distance of the air gap. Thus, the variation of the air gap distance can be calculated by the equations:

$$g_{max} = \left(\sum V_x - \sum V_y\right) + Tt \tag{16}$$

$$g_{min} = \left(\sum V_x - \sum V_y\right) - Tt \tag{17}$$

where g_{max} is the maximum air gap distance and g_{min} is the minimum air gap distance.

E. Tolerance resizing/value re-allocation process

This tolerance accumulation analysis process is repetitive. The process of re-allocating/resizing the tolerance value of each component feature will continue to be carried out until the tolerance accumulation value in the air gap that meets the allowable requirements is obtained.

The resizing method is carried out in order of priority in accordance with the consideration of the level of ease of the manufacturing process. The priority of resizing the tolerance value is carried out on the component features sequentially in Table 5.

III. Results and Discussions

Based on the fits type between the features of the components and the type of geometry tolerance allocated to the component features as well as considering the capabilities of the production machine, the dimensional tolerance values and the initial geometry of the features are allocated, which are shown in Table 6.

From the initial tolerance allocation value, the calculation process for each variable value and tolerance as well as the accumulated tolerance value for the air gap is carried out. The calculation results from the initial allocation can be seen in Table 7. The minimum air gap distance value is 0.612 mm and the maximum is 1.335 mm, where this value does not meet the allowable air gap distance requirements.
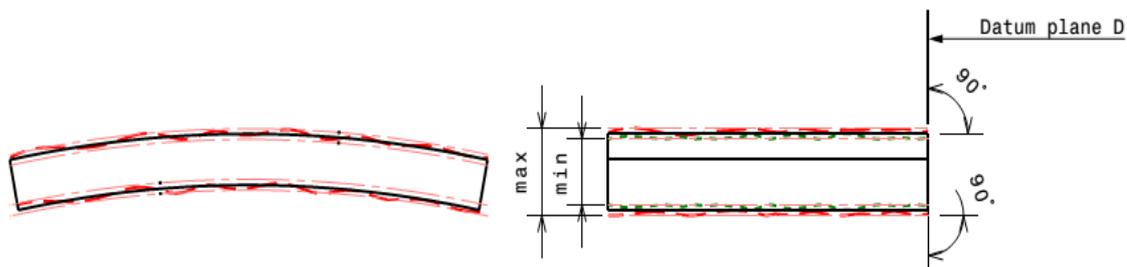
Figure 15. Magnet features deviation simulation

Table 6.
Initial allocation value of tolerance

Component	Features	Nominal dimension (mm)	Dimension tolerance (mm)		Geometry tolerance (mm)				
			(t)		Coaxciality	Cylindricity	Profile	Runout	Total runout
			(t)	(t')	(coax)	(cyl)	(surf)	(ro)	(tro)
Stator	SOS	Ø400	0	-0,02	—	0,02	—	—	—
	SIS	Ø337	0,05	-0,05	0,03	0,02	—	—	—
Shaft	FSBS-SRBS	Ø75	0,015	0,002	0,01	0,02	—	—	—
Rotor	RPMS	Ø323	0,05	-0,05	0,01	—	—	—	0,02
Magnet	MOS	R167,5	0,025	0,025	—	—	0,02		
	MBS	R161,5	0,025	0,025	—	—	0,02		
Bearing	OBS	Ø130	0	-0,018	—	—	—	0,025	—
	IBS	Ø75	0	-0,015	—	—	—	0,015	—
Frame	FSF	Ø412	0,013	0,07	0,03	0,02	—	—	—
	SSF	Ø400	0,06	0	0,03	0,02	—	—	—
End-Shield	FSE	Ø412	0	-0,06	0,03	0,02	—	—	—
	BSE	Ø130	0,04	0	0	0,01	—	—	—

Table 7.
Calculation of the initial tolerance allocation

Variable	Down vector (-) (mm)	Up vector (+) (mm)	Equal bilateral tolerance (mm)	Component
A	31,4875		0,0575	Stator
B	5,99825		0,05625	Frame
C		140,9825	0,0475	End-Shield
D		27,49925	0,02825	Bearing
E		37,50675	0,01575	Shaft
F	161,5025		0,0625	Rotor
G	6		0,07	Magnet
Total	204,98825	205,9885	0,33775	
Maximum air gap (mm)			1,338	
Minimum air gap (mm)			0,6625	

The re-allocation/resizing process of tolerance values is carried out in order of priority in accordance with the consideration of the level of ease of the manufacturing process in Table 5. Figure 16 shows a graph of the resizing process of component feature tolerance allocation values. The first iteration shows the initial allocation value and in the last iteration, the final allocation value is obtained, where the accumulated air gap distance is obtained in accordance with the permit requirements. Figure 17 shows the process of changing the value of the maximum and minimum air gap variations in accordance with the resizing process/changes in the allocated tolerance value.

The final tolerance value allocated to each contributor component feature can be seen in Table 8, while the results of the calculation of the final tolerance allocation can be seen in Table 9. The value of the variation of the air gap distance has met the requirements, namely 1.1785 mm for the maximum value and 0.8 mm for the minimum value.

The evaluation of the final result of the tolerance value allocation is that the smallest tolerance value allocated is 1 μ m for the shaft FSBS/SRBS feature and
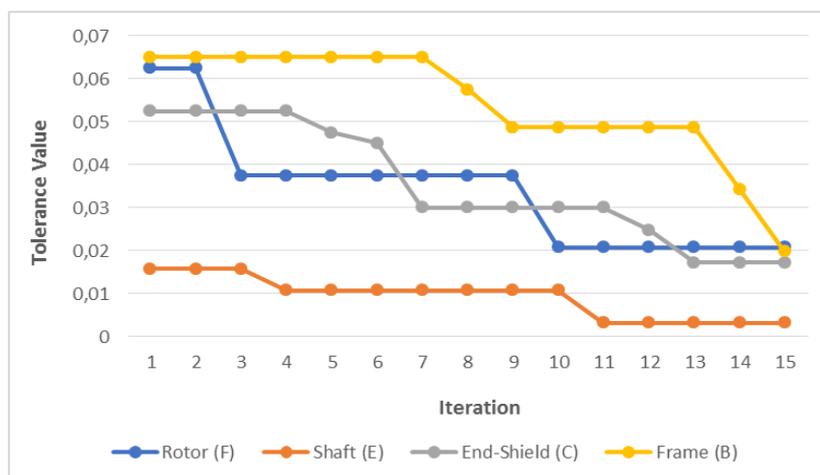
Figure 16. Tolerance value resizing process
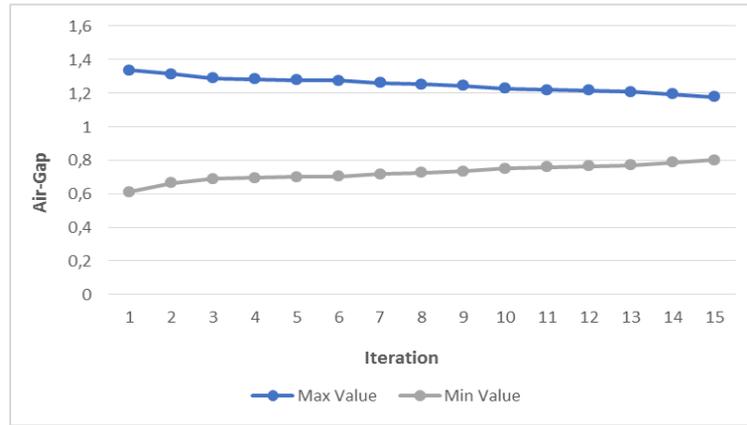
Figure 17. The process of calculating the value of the accumulated air-gap tolerance variation

Table 8.
Final tolerance allocation value

Component	Features	Nominal dimension (mm)	Dimension tolerance (mm)		Geometry tolerance (mm)				
			(t)		Coaxciality	Cylindricity	Profile	Runout	Total runout
			(t)	(t')	(coax)	(cyl)	(surf)	(ro)	(tro)
Stator	SOS	Ø400	0	-0,02	—	0,02	—	—	—
	SIS	Ø337	0,02	-0,02	0,02	0,02	—	—	—
Shaft	FSBS-SRBS	Ø75	0,02	0,01	0,001	0,001	—	—	—
Rotor	RPMS	Ø323	0,02	0,02	0,001	—	—	—	0,001
Magnet	MOS	R167,5	0,02	0,02	—	—	0,02		
	MBS	R161,5	0,02	0,02	—	—	0,02		
Bearing	OBS	Ø130	0	-0,018	—	—	—	0,025	—
	IBS	Ø75	0	-0,015	—	—	—	0,015	—
Frame	FSF	Ø412	-0,014	0	0,004	0,004	—	—	—
	SSF	Ø400	0,06	-0,039	0,004	0,004	—	—	—
End-Shield	FSE	Ø412	0	-0,02	0,003	0,003	—	—	—
	BSE	Ø130	0,02	-0,02	0	0,005	—	—	—

Table 9.
Calculation of the final tolerance allocation

Variable	Down vector (-) (mm)	Up vector (+) (mm)	Equal bilateral tolerance (mm)	Component
A	31,49		0,04	Stator
B	6,02075		0,01975	Frame
C		140,99325	0,01725	End-Shield
D		27,49925	0,02825	Bearing
E		37,50775	0,00325	Shaft
F	161,50025		0,02075	Rotor
G	6		0,06	Magnet
Total	205,011	206,00025	0,18925	
Maximum air gap (mm)			1,1785	
Minimum air gap (mm)			0,8	

the rotor RPMS feature. With this tolerance value, the required manufacturing process is the finishing process from grinding to polishing. The results obtained from this method, when compared with the known WC method, are still the same. However, when compared to the ease of determining which geometric tolerances influence/contribute to KC, this method is easier to determine, that is by simulating the component feature deviation due to the allocated geometry tolerance. In addition, with this method, the required manufacturing process can be known earlier during the tolerance value allocation process by considering the machine's capabilities. Meanwhile, compared to statistical-based methods,

the results of calculations using this method have a greater total accumulated value. However, as it is known that the weakness of the statistical method to calculate the total tolerance value, namely the possibility of defective products, will be greater than using the WC-based method.

IV. Conclusion

This paper has presented a method used to determine and allocate tolerances in designing a prototype component of a radial flux type permanent magnet generator. The calculations and simulations results show that with an air gap of 1 ±

0.2 mm, the maximum air gap value obtained is 1.1785 mm and the minimum is 0.8 mm. The smallest tolerance value allocation is 1 μm on the shaft precisely on the FSBS/SRBS feature and the rotor on the RPMS feature. The manufacturing finishing process needed to achieve the smallest tolerance value on the component features is grinding, lapping, and polishing processes.

Acknowledgment

Declarations

Author contribution

Muhammad Fathul Hikmawan contributed as the main contributor of this paper. All authors read and approved the final paper.

Funding statement

Conflict of interest

The authors declare no known conflict of financial interest or personal relationships that could have appeared to influence the work reported in this paper.

Additional information

Reprints and permission information is available at https://mev.lipi.go.id/.

Publisher's Note: Research Centre for Electrical Power and Mechatronics - Indonesian Institute of Sciences remains neutral with regard to jurisdictional claims and institutional affiliations.

References

[1] N. Harkati, L. Moreau, M. Zaim, and J. F. Charpentier, "Low speed doubly salient permanent magnet generator with passive rotor for a tidal current turbine," in *2013 International Conference on Renewable Energy Research and Applications (ICRERA)*, 2013, pp. 528-533.

[2] L. Wei, T. Nakamura, and K. Imai, "Development and optimization of low-speed and high-efficiency permanent magnet generator for micro hydro-electrical generation system," *Renewable Energy*, vol. 147, pp. 1653-1662, 2020.

[3] A. Al-Adsani and N. Schofield, "Hybrid permanent magnet generators for electric vehicle applications," in *2009 IEEE International Electric Machines and Drives Conference*, 2009, pp. 1754-1761.

[4] T. d. P. M. Bazzo, J. F. Kölzer, R. Carlson, F. Wurtz, and L. Gerbaud, "Multiphysics design optimization of a permanent magnet synchronous generator," *IEEE Transactions on Industrial Electronics*, vol. 64, pp. 9815-9823, 2017.

[5] H. Z. Agrebi, N. Benhadj, M. Chaieb, F. Sher, R. Amami, R. Neji, *et al.*, "Integrated optimal design of permanent magnet synchronous generator for smart wind turbine using genetic algorithm," *Energies*, vol. 14, p. 4642, 2021.

[6] D.-K. Lim, S.-Y. Jung, K.-P. Yi, and H.-K. Jung, "A novel sequential-stage optimization strategy for an interior permanent magnet synchronous generator design," *IEEE Transactions on Industrial Electronics*, vol. 65, pp. 1781-1790, 2017.

[7] P. Irasari, H. S. Alam, and M. Kasim, "Analytical design method of 3 KW, 200 rpm permanent magnet generator for renewable energy power plant applications," *Ketenagalistrikan dan Energi Terbarukan*, vol. 12, pp. 55-66, 2013.

[8] A. Abdoos, M. Moazzen, and S. Hosseini, "Optimal design of an exterior-rotor permanent magnet generator for wind power applications," *Journal of Operation and Automation in Power Engineering*, 2020.

[9] R. Iracheta-Cortez, W. Durante-Gomez, and J. Dorrego-Portela, "Designing a radial-type multi-pole permanent magnet synchronous generator (PMSG) for horizontal axis wind turbines," in *2017 IEEE 37th Central America and Panama Convention (CONCAPAN XXXVII)*, 2017, pp. 1-9.

[10] G. Ombach and J. Junak, "Design of PM brushless motor taking into account tolerances of mass production-six sigma design method," in *2007 IEEE Industry Applications Annual Meeting*, 2007, pp. 2139-2146.

[11] H. Khreis, A. Deflorio, K. Voelz, and B. Schmuelling, "Sensitivity analysis on electrical parameters for permanent magnet synchronous machine manufacturing tolerances in EV and HEV," in *2016 IEEE Transportation Electrification Conference and Expo (ITEC)*, 2016, pp. 1-5.

[12] D. Palani, Z. Azar, A. Thomas, Z. Zhu, and D. Gladwin, "Modeling technique for large permanent magnet generators accounting for manufacturing tolerances and limitations," in *2016 XXII International Conference on Electrical Machines (ICEM)*, 2016, pp. 452-458.

[13] P. Eklund and S. Eriksson, "Air gap magnetic flux density variations due to manufacturing tolerances in a permanent magnet synchronous generator," in *2016 XXII International Conference on Electrical Machines (ICEM)*, 2016, pp. 93-99.

[14] J. Ou, Y. Liu, R. Qu, and M. Doppelbauer, "Experimental and theoretical research on cogging torque of PM synchronous motors considering manufacturing tolerances," *IEEE Transactions on Industrial Electronics*, vol. 65, pp. 3772-3783, 2017.

[15] W. P. Syam, "Toleransi dimensi dan geometri-Analisis rantai variasi dalam proses perakitan produk," *INA-Rxiv*, July 2, 2019.

[16] T. Pyzdek, *The six sigma project planner a step-by-step guide to leading a six sigma project through DMAIC*, McGraw-Hilll Education, 1st edition, April 22, 2003.

[17] A. F. Shukur, N. S. Chin, S. Norhayati, and B. N. Taib, "Design and optimization of valveless micropumps by using genetic algorithms approach," *Journal of Engineering Science and Technology*, vol. 10, pp. 1293-1309, 2015.

[18] G. Chongying, L. Jianhua, and J. Ke, "Efficient statistical analysis of geometric tolerances using unified error distribution and an analytical variation model," *The International Journal of Advanced Manufacturing Technology*, vol. 84, pp. 347-360, 2016.

[19] S. Khodaygan and M. Movahhedy, "A comprehensive fuzzy feature-based method for worst case and statistical tolerance analysis," *International Journal of Computer Integrated Manufacturing*, vol. 29, pp. 42-63, 2016.

[20] Y.-K. Kim, J.-P. Hong, and J. Hur, "Torque characteristic analysis considering the manufacturing tolerance for electric machine by stochastic response surface method," *IEEE Transactions on Industry Applications*, vol. 39, pp. 713-719, 2003.

[21] C. Renzi, A. Ceruti, and F. Leali, "Integrated geometrical and dimensional tolerances stack-up analysis for the design of mechanical assemblies: an application on marine engineering," *Computer-Aided Design and Applications*, vol. 15, pp. 631-642, 2018.

[22] I. Djodikusumo, K. Suherman, and P. B. A. Oken, "Tolerance Stack Analysis in Francis Turbine Design," *Journal of Engineering and Technological Sciences*, vol. 42, pp. 73-90, 2010.

[23] M. Ashby, "*Processes and Process Selection, Materials Selection in Mechanical Design*," ed: Elsevier Ltd, Amsterdam, 2011.

[24] N. Catalogue, "Ball and Roller Bearings," NTN Corporation, 2001.